Desensitization of NMDA Receptor Channels Is Modulated by Glutamate Agonists

Rinat Nahum-Levy, Dafna Lipinski, Sara Shavit, and Morris Benveniste

Department of Physiology and Pharmacology, Sackler School of Medicine, Tel Aviv University, Ramat Aviv, 69978 Israel

ABSTRACT Two distinct forms of desensitization have been characterized for *N*-methyl-D-aspartate (NMDA) receptors. One form results from a weakening of agonist affinity when channels are activated whereas the other form of desensitization results when channels enter a long-lived nonconducting state. A weakening of glycine affinity upon NMDA receptor activation has been reported. Cyclic reaction schemes for NMDA receptor activation require that a concomitant affinity shift should be observed for glutamate agonists. In this study, measurements of peak and steady-state NMDA receptor currents yielded EC_{50} values for glutamate that differed by 1.9-fold, but no differences were found for another agonist, L-cysteine-S-sulfate (LCSS). Simulations show that shifts in EC_{50} values may be masked by significant degrees of desensitization resulting from channels entering a long-lived nonconducting state. Simulations also show that a decrease in the degree of desensitization with increasing agonist concentration is a good indicator for the existence of desensitization resulting from a weakening of agonist affinity. Both glutamate and LCSS exhibited this trend. An affinity difference of three- to eightfold between high-and low-affinity agonist-binding states was estimated from fitting of dose-response data with models containing both types of desensitization. This indicates that activation of NMDA receptors causes a reduction in both glutamate and glycine affinities.

INTRODUCTION

N-methyl-D-aspartate (NMDA) receptor ion channels are one of the postsynaptic targets of glutamate-mediated synaptic transmission in the mammalian brain. NMDA receptors play a key role in physiological processes such as development and modification of synaptic plasticity by allowing glutamate-gated calcium influx into neuronal cells (for review see Dingledine et al., 1999; Ozawa et al., 1998). For channel opening to be achieved, NMDA receptor channels require the binding of two different types of agonist: glutamate and glycine (Kleckner and Dingledine, 1988). Activation of NMDA receptors that have been pre-equilibrated with glycine, by a pulse of nearly saturating NMDA (100 μM) produced a peak current that decayed or desensitized to a steady-state level during the NMDA pulse. The degree of desensitization during the NMDA pulse was inversely dependent on the degree of saturation of the glycine-binding site and may result from a weakening of glycine affinity upon channel activation (Benveniste et al., 1990; Mayer et al., 1989; Vyklicky et al., 1990)

Shown below is a simple reaction scheme for NMDA activation (Benveniste et al., 1990) that can explain independent binding of both glutamate- and glycine-binding site agonists and can describe desensitization that can result from a weakening of glycine-binding affinity:

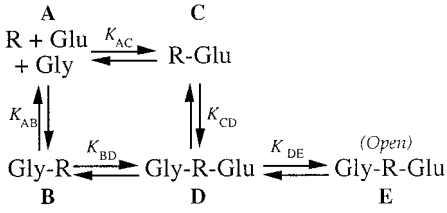

(1)

R represents the receptor, Glu represents the glutamate-binding site agonist (NMDA), Gly represents the glycine-binding site agonist and K_{mn} represents the equilibrium dissociation constants for the transition between states *m* and *n* (states depicted in bold). Provided that $K_{AB} < K_{CD}$, Scheme 1 can simulate the desensitization in the following way. Before NMDA application, NMDA receptors pre-equilibrated with glycine occupy states A and B. When saturating concentrations of NMDA are applied, the reaction scheme shifts rightward toward the open state of the channel (E). At this stage, if glycine concentrations are subsaturating, then a significant number of receptors will occupy states C and D. The desensitization of macroscopic currents can then be explained mechanistically as the re-equilibration of glycine with its low-affinity-state binding site (states C and D) after the sudden switch in receptor occupancy from the higher-affinity states A and B to receptor states C and D, which is induced by NMDA application.

If glycine binding affinities can exist in two affinity states such that K_{AB} is less than K_{CD}, then the law of microscopic reversibility (Colquhoun and Hawkes, 1995) requires that K_{AC} be less than K_{BD} by the same degree. If this is true, then it should be possible to find a type of desensitization that results from a weakening of glutamate-binding affinity. This paper shows that this type of desensitization exists and thus generally reaffirms the basis for a cyclic reaction scheme for NMDA receptor activation, strengthens the ar-

Received for publication 25 April 2000 and in final form 12 February 2001.

Address reprint requests to Dr. Morris Benveniste, Department of Physiology and Pharmacology, Sackler School of Medicine, Tel Aviv University, Ramat Aviv, 69978 Israel. Tel.: 972-3-640-6021; Fax: 972-3-640-9113; E-mail: morrisb@post.tau.ac.il.

0006-3495/01/05/2152/15 $2.00

guments for co-agonist affinity shifts upon receptor activation, and provides a starting point for in-depth study of the reaction scheme for NMDA receptor activation.

MATERIALS AND METHODS

Dissociated neuronal cultures

The procedure for producing low-density rat hippocampal neuronal cultures has been detailed previously (Nahum-Levy et al., 1999). In brief, 14 hippocampi from Sprague-Dawley postnatal day 1 rat pups were digested with papain (100 units; Sigma Chemical Co., St. Louis, MO) for 20 min, triturated to a single-cell suspension, and plated at a density of 75,000 cells/ml onto a 2-week-old glial feeder layer. The glial feeder layer was derived from a similar dissection and grown on a substrate of bovine collagen type IV and 100 μg/ml poly-L-lysine in 35-mm^2 dishes. Glia were maintained in modified Eagle's medium containing 2 mM glutamine, 4.5 g/L D-glucose, 10% fetal bovine serum, 100 U/ml penicillin, and 100 μg/ml streptomycin. Neurons were maintained in a similar growth medium containing 5% horse serum instead of fetal bovine serum and a neuronal supplement N3 (Guthrie et al., 1987). Glial proliferation was arrested by adding 20 μM fluorodeoxyuridine and 51 μM uridine. All cultures were maintained at 36°C in humidified air containing 5% CO_2.

Electrophysiology and rapid perfusion system

Whole-cell voltage clamp experiments were conducted utilizing an Axopatch 200A amplifier (Axon Instruments, Foster City, CA) at room temperature between 1 and 2 weeks after neurons were plated. The extracellular control solution consisted of 160 mM NaCl, 2.5 mM KCl, 0.2 mM $CaCl_2$, 10 mM glucose, 10 mM HEPES, 400 nM tetrodotoxin, 5 μM bicuculline methochloride, and 10 μg/ml phenol red, adjusted to pH 7.3 and 325 mOsm. The intracellular solution consisted of 125 mM $CsMeSO_3$, 15 mM CsCl, 0.5 mM $CaCl_2$, 3 mM $MgCl_2$, 5 mM Cs_4BAPTA, and 2 mM Na_2ATP, adjusted to pH 7.2 and 305 mOsm.

The rapid drug perfusion apparatus has been described in detail previously (Nahum-Levy et al., 1999). Experimental solutions were continuously perfused over the whole neuron from a flow pipe consisting of an array of nine glass barrels (~400 μm o.d.) that was positioned ~100 μm away from the neuronal soma. At a given moment, a stepper motor positioned an adjacent barrel in front of the neuronal soma and a different solution began to flow. The time constant for solution exchange around the neuron (τ_{ex}), has been determined by measuring the current rise from hippocampal neurons elicited by a switch between two solutions containing 150 μM kainate in which the NaCl concentration increases from 5 to 160 mM (Vyklicky et al., 1990). This time constant was ~10 ms. Data were acquired utilizing a Macintosh PPC 7600 computer with an ITC-16 analog-to-digital converter (Instrutech Corp., Port Washington, NY). Synapse, a Macintosh-based electrophysiological software package (Synergistic Systems, Silver Spring, MD) was used for controlling data acquisition and for data analysis.

Although neurons are constantly perfused with an extracellular solution, the hippocampal neuron-glial mixed culture system still secreted a significant amount of glycine agonist to elicit responses to 300 μM NMDA in the absence of added glycine. Responses are similar for concentrations of added glycine ≤100 nM. Application of glutamate in the absence of L-alanine also elicited inward currents. To reduce the possible influence of channels entering desensitized states before the L-alanine pulse, glycine-binding site low-affinity competitive antagonist, 5-methyl-indole-2-carboxylic acid (5MeI2CA) (Huettner, 1989) was added to all solutions containing glutamate but lacking L-alanine. 5MeI2CA reduced the peak response to the application of 10 μM glutamate with no added glycine with an IC_{50} = 1.2 mM and a Hill coefficient of 1.5 (n = 5 cells). For subsequent experiments 10 mM 5MeI2CA was used, which reduced peak responses elicited by the addition of 10 μM glutamate with no added glycine to 1.1 ± 0.6% (n = 5 cells, data not shown) of the control responses in the absence of 5MeI2CA. Low-affinity binding is highly indicative of rapidly dissociating compounds; thus, it was expected that 5MeI2CA would dissociate within the time required for solution exchange. Peak NMDA receptor responses elicited by a pulse of L-alanine in the continual presence of a background concentration of 10 μM glutamate were not reduced; nor was the rise time of the L-alanine response slowed by addition of 10 mM 5MeI2CA to the solutions not containing L-alanine (data not shown).

Dose-response analysis

Standard dose-response analysis was done utilizing the Hill equation:

$$100 \times \frac{I}{I_{p,control}} = 100 \times \frac{I_{max}}{1 + \left(\frac{EC_{50}}{[agonist]}\right)^{n_H}}, \quad (2)$$

where I_{max} is the maximal response, EC_{50} represents the concentration of the half maximal response and n_H is the Hill coefficient. I represents either I_p or I_f, which are the peak and final current amplitudes, respectively. I_p is defined as the maximal amplitude recorded within the first 500 ms of the NMDA receptor response, whereas I_f is an average of the current during the final 200 ms of the NMDA response. Both I_p and I_f must be normalized to a standardized I_p response (i.e., 10 μM for glutamate and 100 μM for LCSS) to compare responses between different experiments. Experimental measurement of the degree of desensitization is:

$$\text{Degree of desensitization} = 1 - \frac{I_f}{I_p}. \quad (3)$$

Note that for this analysis, the degree of desensitization can be determined from I_p and I_f values from each trace without normalization to a standardized response. The degree of desensitization is only determined for those concentrations where the maximal response is not I_f (i.e., a peak response exists). When plotted against agonist concentration, the degree of desensitization can be fitted with an empirical equation of the Hill form:

$$\text{Degree of desensitization} = D_{min} + \frac{D_{max} - D_{min}}{1 + \left(\frac{[agonist]}{CD_{1/2}}\right)^{n_D}} \quad (4)$$

where $CD_{1/2}$ is the concentration at which the degree of desensitization is half maximal. D_{max} and D_{min} are the maximal and minimal degrees of desensitization, respectively. n_D is the Hill coefficient indicative of the slope of the degree-of-desensitization relationship. Errors are standard deviations of the mean.

Simulations and fitting models to data

Whole-cell currents under voltage clamp were simulated by numerical calculations of the probability to occupy open states as described previously (Benveniste et al., 1990). This program was originally written by Dr. J. D. Clements and extensively modified by Benveniste. Exchange between solution conditions was modeled with a 10-ms exchange time constant for all simulations. Parameters for models 1 and 2 (see Fig. 3) were determined by fitting these models simultaneously to average normalized peak and final amplitude data sets as well as the degree-of-desensitization data set. Because the degree of desensitization is theoretically derived from I_p and I_f, inclusion of this data set in the fitting procedure may seem redundant. However, the degree-of-desensitization values were determined independently for each data trace and do not result from utilizing average I_p and I_f values of Fig. 2 C in Eq. 3. In practice, addition of this data set limited the number of solution sets. Model parameters were estimated iteratively utilizing a Simplex algorthim (Press et al., 1992), and the error function was the summation of the square of the difference between the model

estimates and the three data sets (sum squared error (SSE)). The only parameters that were allowed to freely vary during the fitting procedure were k_{1off}, k_{2off}, k_{3off}, and k_{5on} (see Table 2). The data could not be successfully fit with the addition of more freely variable parameters. The following parameters remained constant during the fit, but their values were varied systematically between fits: k_{1on}, k_{3on}, and k_{5off}. Simulations were conducted on a Power Macintosh G3 computer.

RESULTS

Degree of desensitization decreases as the background concentration of glutamate is increased

Applying a pulse of nearly saturating NMDA (300 μM) in the continual presence of glycine to rat cultured hippocampal neurons, elicited NMDA receptor currents that peaked and desensitized (Fig. 1 *A*). I_p and I_f measured during the NMDA pulse increased when the pre-equilibrated background concentration of glycine was increased; however, I_p tended toward saturation at lower background concentrations of glycine in comparison with those required for saturation of I_f (Fig. 1 *A*). This suggests that the affinity for glycine binding at I_p may be higher than that at I_f. The degree of desensitization (Eq. 3) gradually decreases from 64.9 ± 6.3% for responses in which no background concentration of glycine was added (endogenous levels) to 41.2 ± 8.2% (n = 13 cells) in which 10 μM glycine was added (Fig. 1 *B*). Desensitization of currents elicited by 100 μM NMDA in the continual presence of various concentra-

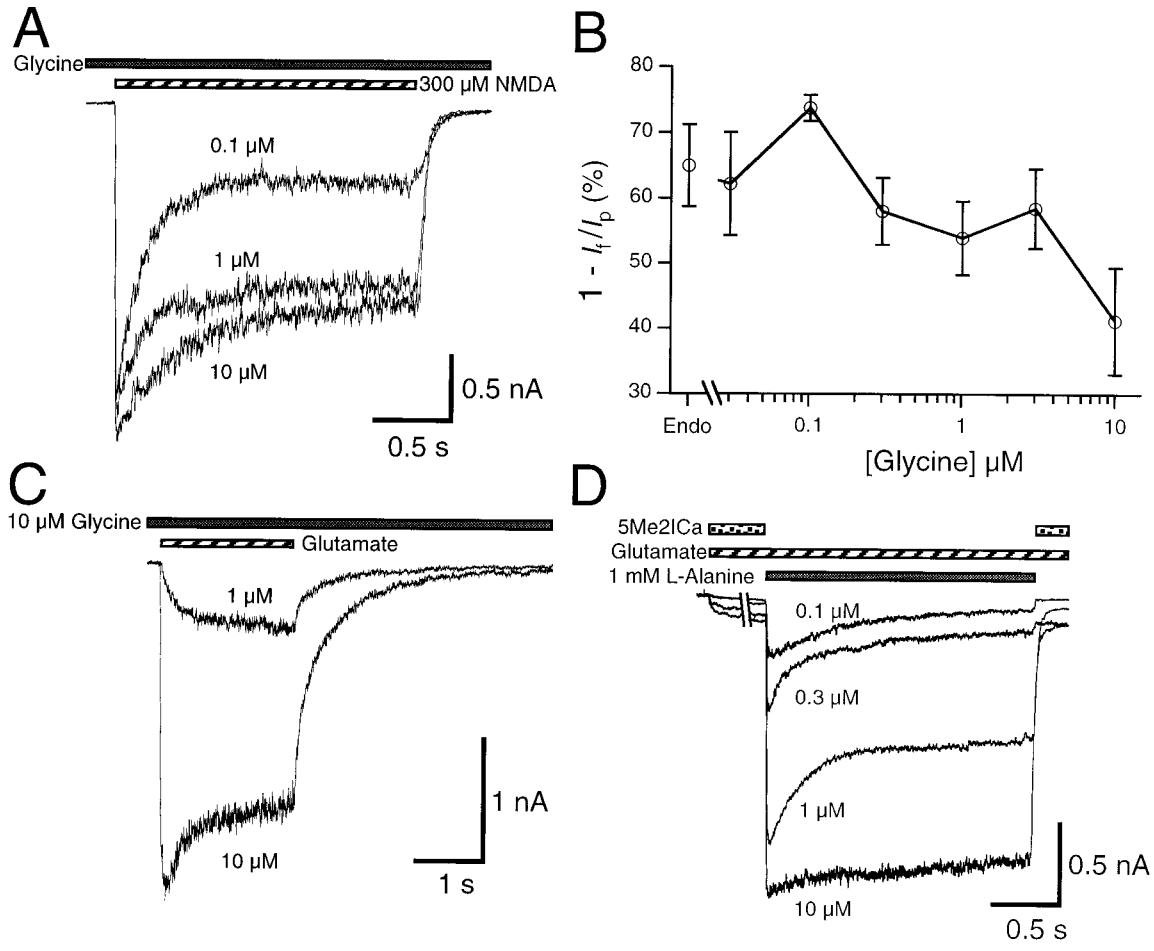

FIGURE 1 NMDA receptors exhibit desensitization whose degree depends on the background concentration of either glycine or glutamate. (*A*) In the same hippocampal neuron, 300 μM NMDA was pulsed for 1.5 s in the continual presence of a background concentration of 0.1, 1, or 10 μM (saturating) added glycine. Current responses desensitized 72.7%, 39.6%, and 37.5%, respectively, indicating a dependence on glycine concentration. (*B*) Plot of the degree of desensitization with changing background glycine concentration. I_p and I_f data were extracted from experiments like that depicted in *A* and subjected to Eq. 3 and show a decreasing degree of desensitization with increasing glycine concentration. Endo indicates the degree of desensitization observed for a 300 μM NMDA pulse with no added (endogenous) glycine. (*C*) When either 1 or 10 μM (saturating) glutamate was pulsed in the continual presence of a 10 μM background concentration of glycine, only the 10 μM glutamate response desensitized (27%). The 1 μM glutamate response nearly reached equilibrium at the end of the 1.5-s glutamate pulse. (*D*) When glutamate and 10 mM 5MeI2CA were pre-equilibrated with neurons before pulsing with 1 mM L-alanine, NMDA receptor responses desensitized. Current traces are from three different cells whose amplitudes have been normalized to the 10 μM glutamate response shown. Currents desensitized 75.1, 68.0, 41.0, and 12.6% for 0.1, 0.3, 1, and 10 μM glutamate. The time gap symbolized by the double backslash is 800 ms.

tions of glycine has been characterized on cultured mouse neurons in more detail previously (Vyklicky et al., 1990).

We wished to determine whether NMDA receptor responses would desensitize to differing degrees by variation of glutamate agonist concentration while the glycine background concentration was held constant near saturation. When applying a pulse of glutamate at concentrations >1 μM in the continual presence of 10 μM glycine, peak currents were observed within the first 500 ms of glutamate application (Fig. 1 *C*). For glutamate concentrations ≤1 μM, NMDA receptor responses increased slowly, such that the maximum amplitude observed during the glutamate application was I_f (Figs. 1 *C* and 2 *A*). The slow rise in NMDA receptor currents observed at these glutamate concentrations probably results from a slow association rate for glutamate binding at low glutamate concentrations. Such a problem can be alleviated by conducting the converse experiment to that of Fig. 1 *A*.

A given constant background concentration of glutamate in the absence of added glycine is allowed to pre-equilibrate with NMDA receptors before their activation with a pulse of a saturating concentration of L-alanine (1 mM), a low-affinity glycine agonist (Fig. 1 *D*). A rapid rise in the NMDA receptor response was observed when a solution of

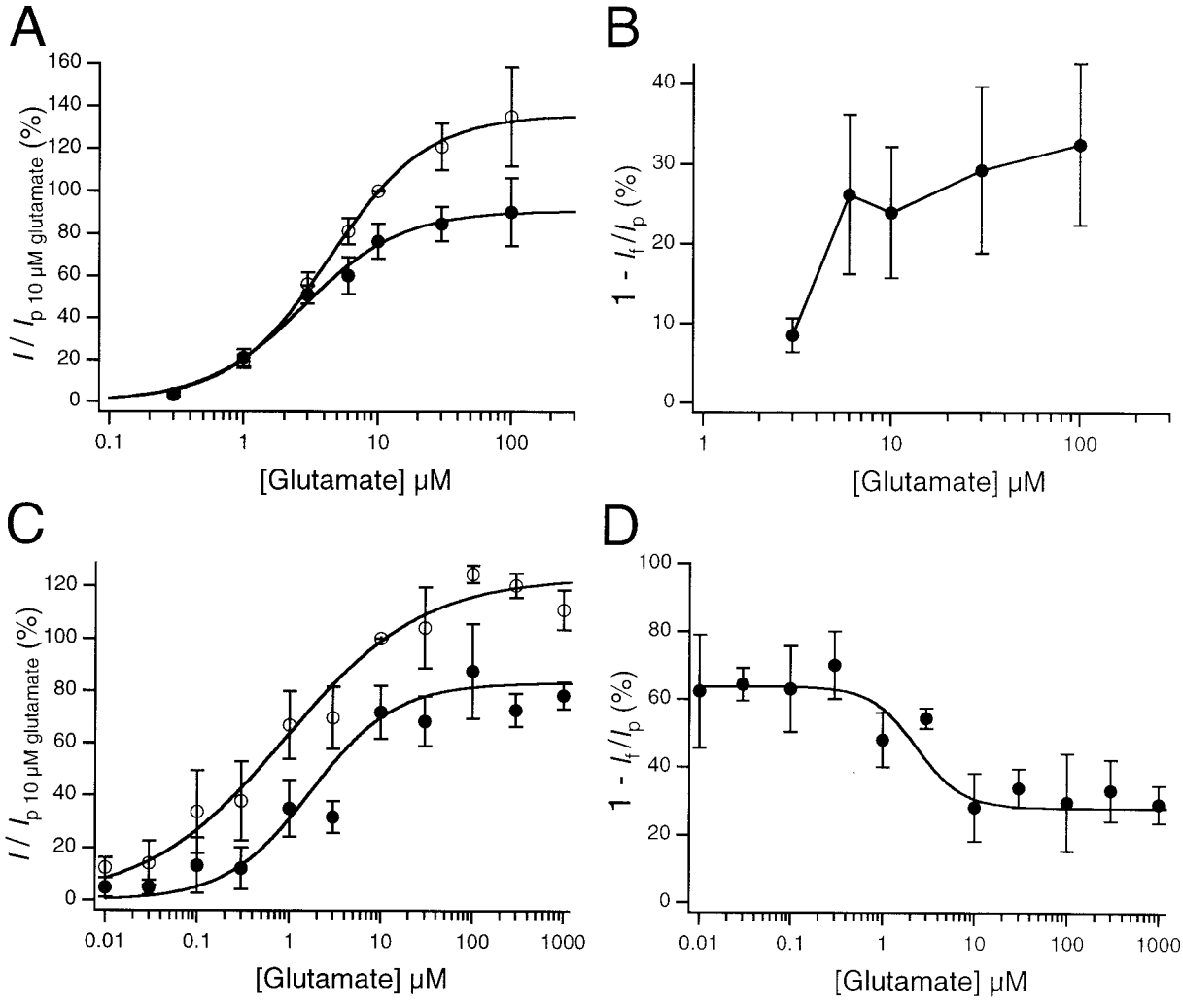

FIGURE 2 Dose-response analysis of desensitizing NMDA receptor responses modulated by glutamate. (*A*) I_p (○) and I_f (●) response amplitudes were measured for NMDA currents elicited with various concentrations of glutamate in the continual presence of 10 μM glycine. Analysis of responses according to Eq. 2 yielded an EC_{50} value of 4.3 ± 0.4 μM and Hill coefficient of 1.2 ± 0.1 for the I_p curve, and an EC_{50} value of 2.8 ± 0.4 μM and Hill coefficient of 1.2 ± 0.1 for the I_f curve (n = 14 cells). (*B*) The degree of desensitization defined by Eq. 3 is plotted with respect to glutamate concentration. Only positive values derived from Eq. 3 are plotted. The plot indicates that desensitization increases as glutamate concentration increases. (*C*) I_p (○) and I_f (●) dose response curves derived from experiments in which 1 mM L-alanine was pulsed in the continual presence of various background concentrations of glutamate. The I_p EC_{50} was 0.9 ± 0.1 μM with an n_H of 0.60 ± 0.03. The I_f EC_{50} was 1.7 ± 0.3 μM with an n_H of 0.9 ± 0.1. I_{max} values for I_p and I_f curves were 123.4 ± 2.6 and 83.1 ± 2.8%, respectively. (*D*) The degree-of-desensitization plot for the experiment depicted in *C* yielded a $CD_{1/2}$ value of 2.3 ± 0.7 μM, an n_D of 1.8 ± 0.6, and D_{max} and D_{min} values of 63.7 ± 2.6% and 28.0 ± 2.2%, respectively.

1 mM L-alanine and a given background concentration of glutamate replaced a solution containing 10 mM 5MeI2CA, and the same background concentration of glutamate. 5MeI2CA was used to inhibit NMDA receptor responses when glutamate was applied alone (see Materials and Methods). Desensitization of the peak current was observed for all background glutamate concentrations used (Fig. 1 *D*); however, the degree of desensitization was markedly lower for background concentrations ≥ 10 μM glutamate than for concentrations ≤ 3 μM glutamate (Fig. 2 *D*).

Dose-response analysis of I_p and I_f for glutamate pulsed at various concentrations in the continual presence of a background concentration of 10 μM glycine (Fig. 1 *C*) yielded EC_{50} values of 4.3 $\pm$ 0.4 μM and 2.8 $\pm$ 0.4 μM, respectively (Fig. 2 *A*), and Hill coefficients for both I_p and I_f = 1.2 $\pm$ 0.1 (n = 14 cells). At glutamate pulse concentrations ≤ 1 μM, the concentration-dependent association of glutamate with NMDA receptors seems to be slower than the kinetics of desensitization, such that no peak currents were observed (Figs. 1 *C* and 2 *A*). Fig. 2 *B* indicates that the degree of desensitization increased with increasing glutamate concentration for those concentrations at which a peak current could be observed (>1 μM).

When a given concentration of glutamate was applied continuously throughout the experiment and a pulse of 1 mM L-alanine applied to elicit NMDA receptor activation (Fig. 1 *D*), I_p and I_f dose-response curves did not generally overlap (Fig. 2 *C*). Analysis of I_p and I_f yielded a small but significant difference in EC_{50} values: 0.9 $\pm$ 0.4 μM for I_p and 1.7 $\pm$ 0.3 μM for I_f (n = 53 cells; $p < 0.0001$). The degree of desensitization measured from currents elicited with this protocol decreased as the background concentration of glutamate increased (Fig. 2 *D*). This is in contrast to the observed increase in the degree of desensitization as the concentration of glutamate increases during the glutamate pulse protocol (Fig. 2 *B*). The data in Fig. 2 *D* were fit with Eq. 4 to yield a $CD_{1/2}$ value of 2.3 $\pm$ 0.7 μM with a n_D of 1.8 $\pm$ 0.6 and limiting desensitization levels of 63.7 $\pm$ 2.6 and 28.0 $\pm$ 2.2% for D_{max} and D_{min}, respectively (n = 53 cells).

Simulations of changes in the degree of desensitization with changing glutamate concentration

Because less than a twofold increase in EC_{50} values was observed between I_p and I_f data in Fig. 2 *C*, we were not convinced that desensitization observed when 1 mM L-alanine was pulsed in the continual presence of glutamate reflected a mechanism in which glutamate affinity is weakened upon glycine agonist binding and channel activation. Other desensitization mechanisms are known to exist (Krupp et al., 1996, 1998, 1999; Legendre et al., 1993; Medina et al., 1995; Sather et al., 1990; Tong and Jahr, 1994). In general, these desensitization phenomena can be described by agonist-bound receptors that enter a long-lived (desensitized) state from which channel activation is not directly possible (i.e., transition 5 in Fig. 3). Such desensitization mechanisms might reduce or mask a shift in glutamate affinities that otherwise would be observed by analysis of I_p and I_f dose-response curves. To test this possibility theoretically, two cyclic models containing two binding sites each for glutamate and glycine agonists were used for simulating NMDA receptor responses (Fig. 3, *A* and *B*). Previous studies have suggested that the binding of two molecules of a glycine agonist and two molecules of a

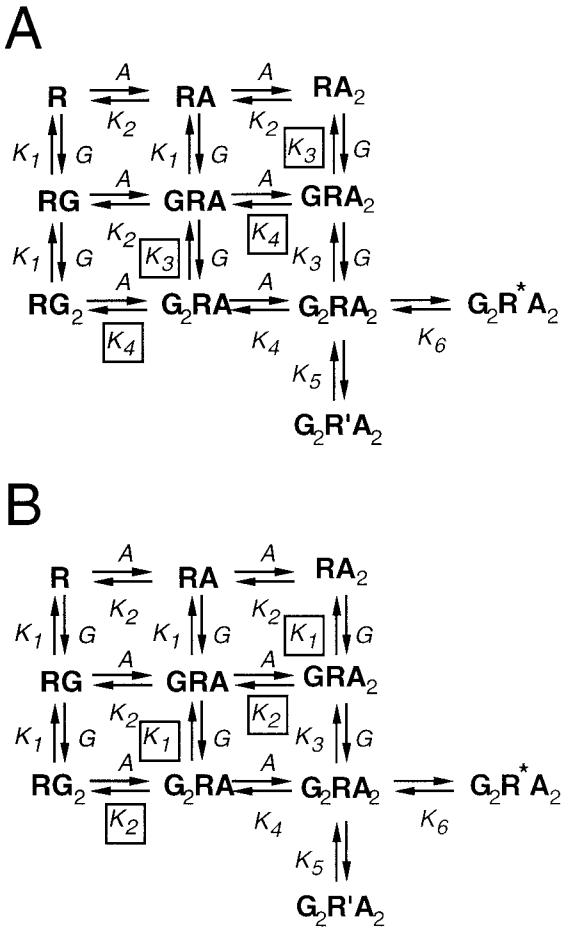

FIGURE 3 Reaction schemes for two models containing two binding sites for each agonist. Model 1 (*A*) and model 2 (*B*) require the binding of two molecules of glutamate (G) and L-alanine (*A*) to reach a fully liganded state (G_2RA_2), which leads to the open state ($G_2R^*A_2$) of the channel. The $G_2R'A_2$ state is the long-lived nonconducting state. The two models differ in their placement of equivalent reactions. K_n represents the equilibrium dissociation constant for equivalent transition type n. Model 1 has six high-affinity agonist-binding macroscopic transitions and six low-affinity agonist-binding macroscopic transitions; whereas model 2 has all high-affinity agonist-binding macroscopic transitions except for the two transitions closest to the fully liganded state. Boxed K_n values emphasize the transitions that differ in their equivalent transition type between the two models. Kinetic parameters utilized for these two models can be found in Tables 1 and 2.

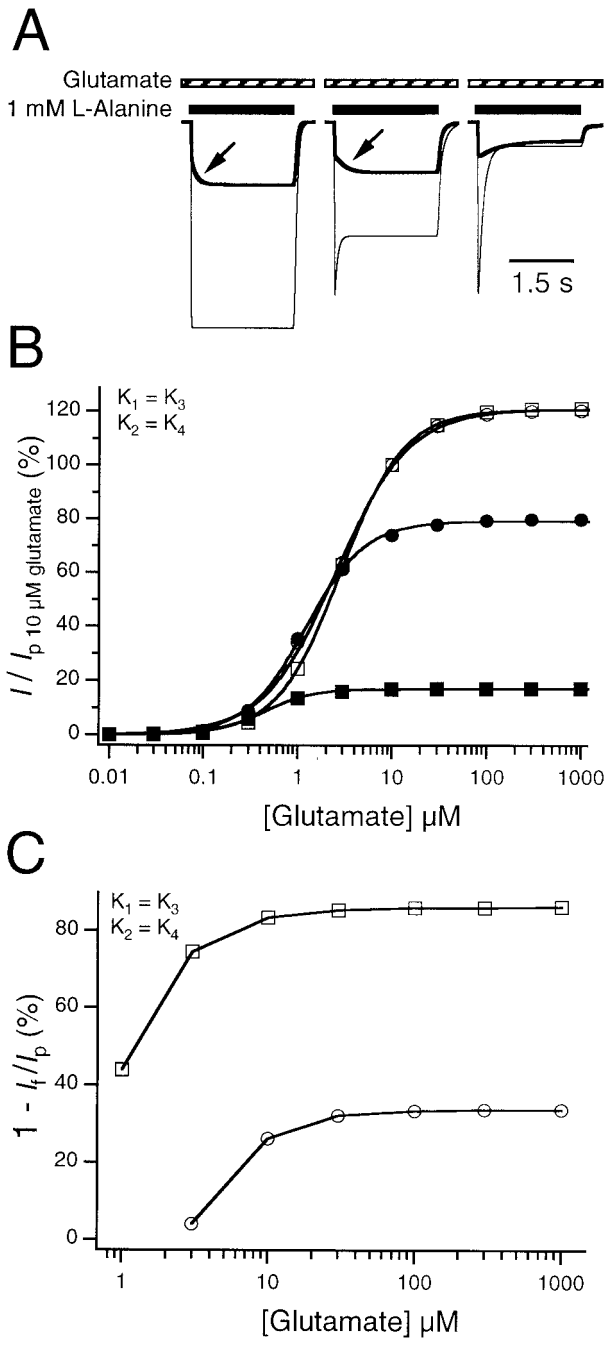

FIGURE 4 Effects of desensitization caused by transition 5 on standard dose-response analysis of models with a single binding affinity for glutamate and L-alanine. Model 1 (Fig. 3 *A*) has been used to simulate NMDA responses resulting from a 1 mM pulse of L-alanine in the continual presence of a given background concentration of glutamate. In all three simulations depicted, models contain a single binding affinity for glutamate and L-alanine such that $K_1 = K_3$ and $K_2 = K_4$. All kinetic parameters are presented in Table 1. (*A*) Simulated currents resulting from three versions of model 1. The left panel contains simulations in which transition 5 had been removed. The middle panel contains simulations in which transition 5 had a k_{off} value of 9.4 s^{-1}, which yielded a moderate level of desensitization (34%) when the background glutamate concentration was saturating. The right panel contains simulations in which transition 5 had a k_{off} value of 1.0 s^{-1}, which yielded considerable desensitization (86%) when the background glutamate concentration was saturating. Thin and thick lines depict currents in which the background concentration of glutamate was either 1 mM or 1 μM, respectively. Arrows emphasize the slow rise of the current in response to the application of 1 mM L-alanine. (*B*) I_p (*open symbols*) and I_f (*filled symbols*) dose-response curves for transition 5 containing models. Circles and squares represent simulations done at discrete glutamate concentrations utilizing the versions of model 1 whose currents are depicted in the middle and right panels of *A*, respectively. Smooth lines indicate the fits to Eq. 2. The model depicted in the middle panel of *A* yielded the following fit parameters: $EC_{50} = 2.6 \pm 0.1$ μM, $n_H = 1.1 \pm 0.1$, and $I_{max} = 120.6 \pm 1.0\%$ for the I_p curve; and $EC_{50} = 1.22 \pm 0.03$ μM, $n_H = 1.4 \pm 0.03$, and $I_{max} = 79.1 \pm 0.5\%$ for the I_f curve (○ and ●). The model shown in the right panel of *A* yielded the following fit parameters: $EC_{50} = 2.9 \pm 0.1$ μM, $n_H = 1.3 \pm 0.02$, and $I_{max} = 120.6 \pm 0.4$ for I_p data; and $EC_{50} = 0.44 \pm 0.01$ μM, $n_H = 1.7 \pm 0.1$, and $I_{max} = 17.0 \pm 0.1\%$ for the I_f data (□ and ■). (*C*) Plot of the degree of desensitization with respect to glutamate concentration for data resulting from the model utilized in the middle panel (○) or right panel of *A* (□). Data points are connected by lines to emphasize the trend of an increasing degree of desensitization with an increasing concentration of background glutamate. Only positive values calculated from Eq. 3 for the degree of desensitization are depicted.

glutamate agonist are required for channel opening (Benveniste et al., 1990; Benveniste and Mayer, 1991; Clements and Westbrook, 1991; Clements and Westbrook, 1994; Rosenmund et al., 1998). These models could simulate desensitization resulting from channels in which agonist affinities weaken upon binding of the co-agonist by setting $K_3 > K_1$ and $K_4 > K_2$. In addition, these models also could simulate desensitization resulting from channels in the fully liganded state that enter a long-lived closed state ($G_2R'A_2$ in Fig. 3).

In Fig. 4, I_p, I_f, and the degree of desensitization are analyzed for model 1 in which the K_5 transition kinetics are altered while the agonist-binding transitions are not weakened by the binding of co-agonist (i.e., $K_3 = K_1$ and $K_4 = K_2$). The kinetic rate constants of the transitions for glutamate binding, channel opening, and the transition into the desensitized state are based on measurements and analysis of NMDA EPSC data utilizing a two-equivalent-site model (Lester and Jahr, 1992). Rate constants for L-alanine were also determined previously (Benveniste and Mayer, 1991). Rate constants for these simulations are presented in Table 1. The simulated protocol is similar to the experimental protocol utilized in Fig. 1 *D*, in which the cell is preequilibrated with a background concentration of glutamate before the addition of 1 mM L-alanine. Fig. 4 *A* shows simulated traces of subsaturating (1 μM) and supersaturating (1 mM) background concentrations of glutamate for a model lacking transition 5 (symbolized by the K_5 equilibrium in Fig. 3), a model in which D_{max} is similar to that of experimental data (Fig. 2 *D*), and a model in which D_{max} is 85%. D_{max} was increased by reducing the rate of return from the desensitized state (k_{off}, transition 5; see Table 1). All simulations were done with the same number of channels, thus allowing direct comparison of I_p and I_f between

TABLE 1 Rate constants for simulations of NMDA receptor activation utilizing model 1

Transition*	Agonist	k_{on} (μM^{-1} s^{-1})	k_{off} (s^{-1})	k_{off}/k_{on}
1	Glutamate			
	Fig. 4	5.0†	6.7‡	1.3 μM
	Fig. 5	5.0†	1.68	0.34 μM
	Fig. 6	5.0†	0.84, 1.68, 3.36	0.17, 0.34, 0.67 μM
2	L-Alanine			
	Fig. 4	1.7§	19.9§	11.7 μM
	Fig. 5	1.7§	2.48, 4.95, 9.95	1.46, 2.91, 5.85 μM
3	Glutamate			
	Figs. 4–6	5.0†	6.7‡	1.3 μM
4	L-Alanine			
	Figs. 4–6	1.7§	19.9§	11.7 μM
5¶	Agonist independent‖			
	Figs. 4 and 5	15.2‡	1.0, 9.4‡	0.07, 0.62
	Fig. 6	15.2‡	1, 2, 4, 8, 16, 32	0.07, 0.13, 0.26, 0.53, 1.05, 2.11
6	Agonist independent‖			
	Figs. 4–6	83.8‡	83.8‡	1.0

*Equivalent transition types are numbered according to the scheme depicted in Fig. 3 *A* (model 1).
†Taken from Clements and Westbrook (1991).
‡Taken from NMDA EPSC data of Lester and Jahr (1992).
§Taken from Benveniste and Mayer (1991).
¶This transition is omitted in the simulations presented in the left panel of Figs. 4 *A* and 5 *A*.
‖Agonist-independent k_{on} are in units of s^{-1}.

each of the three models shown (Fig. 4 *A*). When transition 5 was omitted, simulated responses did not desensitize (Fig. 4 *A*, left panel), and the magnitude of the response was greater than when transition 5 was included in model 1 (Fig. 4 *A*, middle and right panels). Responses in which a peak current was observed were at glutamate concentrations of 1–3 μM (Fig. 4 *B*). At lower background glutamate concentrations, the rise in the simulated responses had a slow phase (arrows, Fig. 4 *A*), such that I_p measured within the first 500 ms of L-alanine application was $\leq I_f$ (Fig. 4 *B*). The slow rise in the simulated response at these concentrations was unexpected because the background glutamate concentrations are pre-equilibrated with their receptors before the 1 mM L-alanine application. For the two simulations in which transition 5 was included, the degree of desensitization increased as glutamate concentrations were increased (Fig. 4 *C*). Similar trends were also observed for model 2 (data not shown).

To simulate desensitization caused by a weakening of agonist affinity, model 1 was set such that K_3 was fourfold greater than K_1 (and hence K_4 was fourfold greater than K_2) for the following simulations. As in Fig. 4, background concentrations of 1 μM and 1 mM glutamate were pre-equilibrated with their binding sites before application of 1 mM L-alanine (Fig. 5 *A*). The number of channels is equivalent to that used in Fig. 4 to allow direct comparison between the models. When transition 5 was omitted, it can be observed that responses to L-alanine in the presence of saturating glutamate (1 mM) did not desensitize (Fig. 5 *A*, left panel). Yet when a subsaturating background concentration of 1 μM glutamate was used, the response desensitized 38%. In fact, I_p was greater than I_f for all background glutamate concentrations >30 nM (Fig. 5 *B*). In addition, a rightward shift between I_p and I_f dose-response curves is readily apparent (Fig. 5 *B*). Dose-response analysis according to Eq. 2 for the version of model 1 lacking transition 5 yielded EC_{50} values of 1.1 and 1.9 μM for I_p and I_f curves, respectively. Respective Hill coefficients were 1.0 and 1.3. Similar trends were observed in simulations utilizing model 2 (data not shown). The degree of desensitization calculated from I_p and I_f for this version of model 1 was analyzed by Eq. 4. The $CD_{1/2}$ value was 1.8 μM with a Hill coefficient n_D of 1.4. D_{min} and D_{max} values were 0% and 84.3%, respectively. Note that in this simulation (Fig. 5 *A*, left panel), the maximum degree of desensitization (D_{max}) is observed at low glutamate concentrations (Fig. 5 *C*), whereas in the simulations presented in Fig. 4, D_{max} was observed at saturating background glutamate concentrations.

The version of model 1 that contained the fourfold difference between K_1 and K_3 (or K_2 and K_4) was then modified to include transition 5 to characterize the effects of inclusion of both types of desensitization mechanisms on the dose-response analysis. By comparing Fig. 4 *A* with Fig. 5 *A*, it can be observed that for a saturating concentration of glutamate (1 mM), the simulated responses overlap. However, in contrast to Fig. 4 *A*, all subsaturating responses did peak within the first 500 ms of the response (Fig. 5 *A*). Dose-response analysis of data from the simulation in which 1 mM glutamate yielded a moderate degree of desensitization (Fig. 5 *A*, middle panel) produced EC_{50} values of 1.0 and 1.2 μM with Hill coefficients of 1.1 and 1.4 for I_p and I_f, respectively. The degree of desensitization for this sim-

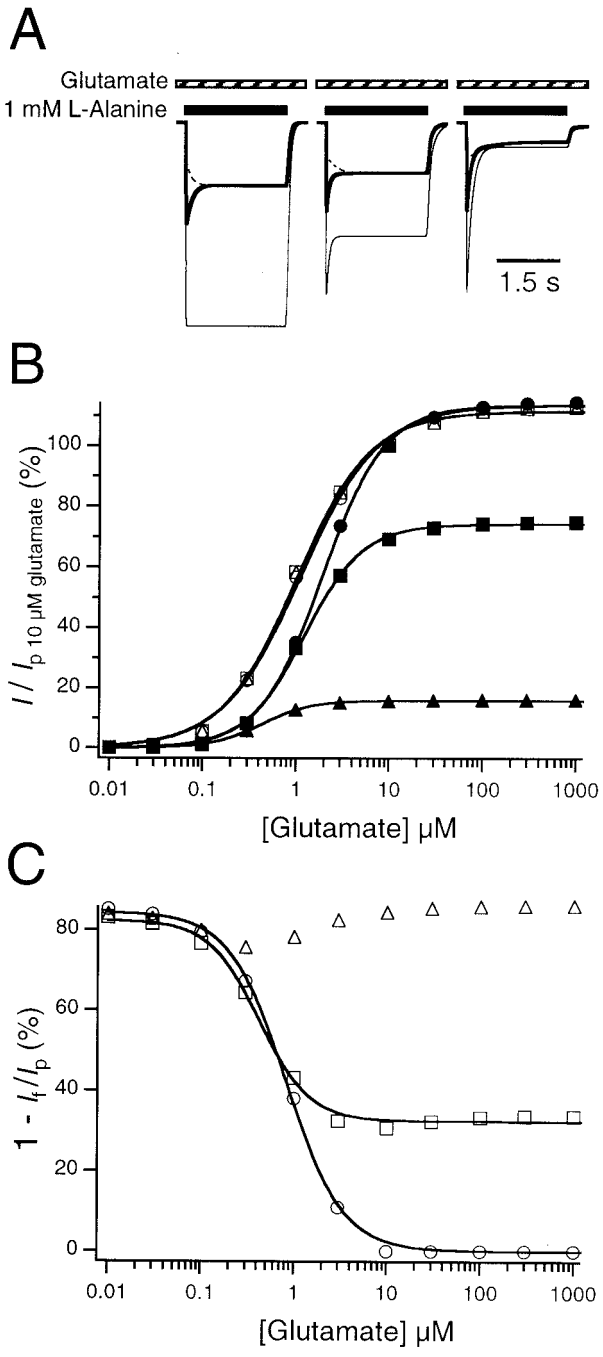

FIGURE 5 Effects of desensitization caused by transition 5 on standard dose-response analysis of models containing high and low agonist affinities for glutamate and L-alanine. Model 1 (Fig. 3 *A*) was used to simulate NMDA responses resulting from a 1 mM pulse of L-alanine in the continual presence of a given background concentration of glutamate. In all three simulations depicted, models contain a fourfold difference between high- and low-affinity binding transitions for glutamate and L-alanine such that $4K_1 = K_3$ and $4K_2 = K_4$. All kinetic parameters are presented in Table 1. (*A*) Simulated currents resulting from three versions of model 1. The left panel contains simulations in which transition 5 had been removed. The middle panel contains simulations in which transition 5 had a k_{off} value of 9.4 s^{-1}, and the right panel contains simulations in which transition 5 had a k_{off} value of 1.0 s^{-1}. Thin and thick lines depict currents in which the background concentration of glutamate was either 1 mM or 1 μM, respectively. Dashed lines depict the same responses to 1 μM glutamate shown in Fig. 4 *A* with $K_1 = K_3$ and $K_2 = K_4$. Currents resulting from simulation of models in Fig. 4 with 1 mM glutamate and 1 mM L-alanine were identical to thin lined responses shown here. (*B*) I_p (*open symbols*) and I_f (*filled symbols*) dose-response curves for the models whose simulations are presented in *A*. Circles, squares, and triangles represent simulations done at discrete glutamate concentrations utilizing the versions of model 1 whose currents are depicted in the left, middle, and right panels of *A*, respectively. Following are the parameters from fits to Eq. 2 (*smooth lines*). For the model not containing transition 5, fit parameters for I_p data were $EC_{50} = 1.1 \pm 0.1$ μM, $n_H = 1.0 \pm 0.1$, and $I_{max} = 113.3 \pm 1.2\%$; fit parameters for I_f data were $EC_{50} = 1.9 \pm 0.1$ μM, $n_H = 1.3 \pm 0.04$, and $I_{max} = 113.4 \pm 0.7\%$ (○ and ●). For the model depicted in the middle panel of *A*, fit parameters for I_p data were $EC_{50} = 1.0 \pm 0.1$ μM, $n_H = 1.1 \pm 0.1$, and $I_{max} = 113.3 \pm 1.1\%$; fit parameters for I_f data were $EC_{50} = 1.2 \pm 0.03$ μM, $n_H = 1.4 \pm 0.1$, and $I_{max} = 74.1 \pm 0.4\%$ (□ and ■). For the model depicted in the right panel of *A*, fit parameters for I_p data were $EC_{50} = 1.0 \pm 0.1$ μM, $n_H = 1.1 \pm 0.1$, and $I_{max} = 111.3 \pm 1.1\%$; fit parameters for I_f were $EC_{50} = 0.4 \pm 0.01$ μM, $n_H = 1.7 \pm 0.04$, and $I_{max} = 15.9 \pm 0.1\%$ (△ and ▲). (*C*) Plot of the degree of desensitization with respect to glutamate concentration for the three versions of model 1 examined in *A*. Fits to Eq. 4 are depicted by smooth lines. Open circles depict analysis done for the model represented in the left panel of A in which transition 5 has been omitted. Fit parameters for this simulation were $CD_{1/2} = 0.8 \pm 0.03$ μM, $n_D = 1.4 \pm 0.1$, $D_{max} = 84.4 \pm 0.8\%$, and $D_{min} = 0.0\%$. Open squares depict analysis done for the model represented in the middle panel of *A*. Fit parameters for this simulation were $CD_{1/2} = 0.4 \pm 0.1$ μM, $n_D = 1.6 \pm 0.2$, $D_{max} = 82.3 \pm 1.1\%$, and $D_{min} = 32.4 \pm 0.6\%$. Open triangles depict analysis done for the model represented in the right panel of *A*. This data could not be fit with Eq. 4.

ulation also decreased with increasing glutamate concentration. Analysis utilizing Eq. 4 yielded a $CD_{1/2}$ value of 0.4 μM with a Hill coefficient n_D of 1.6. D_{min} and D_{max} values were 32.4% and 82.3%, respectively.

Strongly desensitized responses observed from simulations with a saturating concentration of glutamate (Fig. 5 *A*, right panel) result from accumulation of receptors in a high-affinity desensitized state (i.e., $G_2R'A_2$ in Fig. 3). In such a model, the increase in EC_{50} values between I_p and I_f is lost (Fig. 5 *B*), and there is no consistent decrease in the degree of desensitization with increasing glutamate concentration (Fig. 5 *C*). Note that for the strongly desensitizing model (Fig. 5 *A*, right panel) the EC_{50} value for I_p (1.0 μM) was greater than that for I_f (0.4 μM). This contrasts with the experimental result found for I_p and I_f from the glutamate dose response curves (Fig. 2 *C*).

The difference between EC_{50} values determined from I_p and I_f dose-response curves for models where $K_1 < K_3$ (and $K_2 < K_4$) decreases as the desensitized state, $G_2R'A_2$, is stabilized by decreasing K_5 (Table 1 and Fig. 6 *A*). The degree of difference between EC_{50} values for I_p and I_f curves is also model dependent and always underestimates the true difference between high and low agonist binding affinities. When transition 5 does not exist, model 1 yields a 1.7-fold difference between I_p and I_f EC_{50} values, whereas model 2 produces a 1.4-fold difference, even though the ratio of K_3 to K_1 is fourfold (Fig. 6 *A*). When transition 5 is

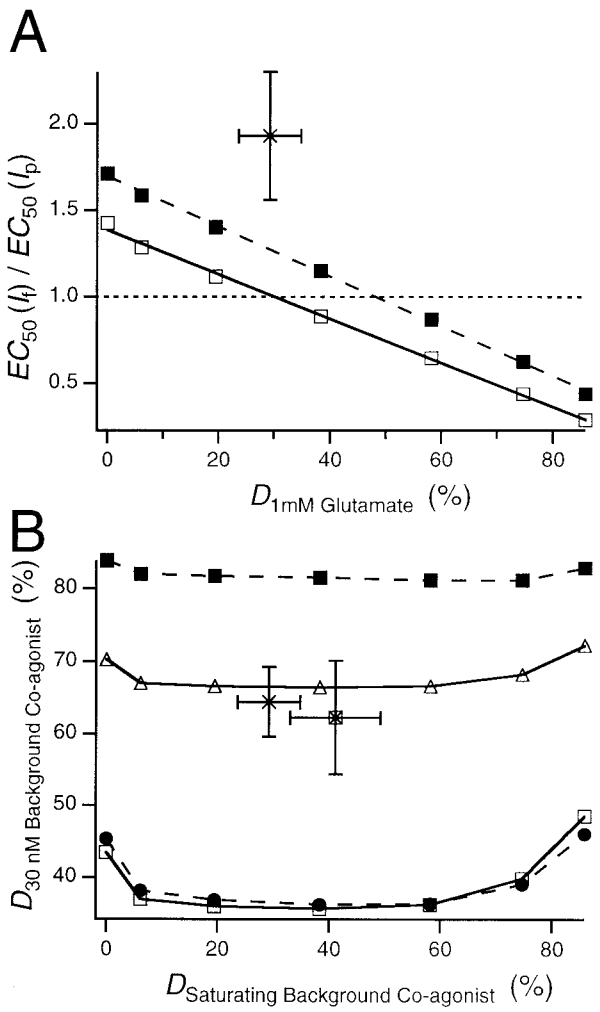

FIGURE 6 Prediction of agonist affinity shifts from dose-response analysis. (*A*) Ratio of EC_{50} values derived from I_p and I_f dose-response curves is plotted with respect to the degree of desensitization observed when the background concentration of glutamate is saturating. The versions of model 1 (■, see Fig. 3 *A*) and model 2 (□, see Fig. 3 *B*) utilized for these simulations contained mechanisms for both types of desensitization, like those utilized in Fig. 5. K_3 was equal to $4K_1$, and K_4 was equal to $4K_2$. k_{off} for transition 5 was varied as shown in Table 1 to yield varying degrees of desensitization when the background glutamate concentration was maximal. The difference between I_p and I_f EC_{50} values dissipates as the degree of desensitization observed at a background concentration of 1 mM glutamate increases. The dashed horizontal line indicates the point at which there is no difference between I_p and I_f EC_{50} values. The ratio of EC_{50} values versus the degree of desensitization derived from experimental data for glutamate (Fig. 2, *C* and *D*) is indicated by the cross-marker. (*B*) Analysis of the degree of desensitization at low and high background agonist concentrations. Models 1 and 2 were simulated utilizing a 1 mM L-alanine pulse and either a 30 nM or 1 mM background concentration of glutamate. The degree of desensitization of the 30 nM glutamate response was plotted against the 1 mM glutamate response for models in which the k_{off} of transition 5 was varied according to Table 1. This procedure was repeated for various ratios of K_1:K_3 (or K_2:K_4). Depicted are ratios of 1:2 for model 1 (●), 1:4 for model 1 (■), 1:4 for model 2 (□), and 1:8 for model 2 (△). Experimental data for glutamate derived from Fig. 2 *D* is also included for comparison (×). Because these models are symmetric, identical data will result from simulations in which glycine is the background agonist, present at either 30 nM or 10 μM concentrations with 300 μM NMDA being pulsed to elicit NMDA receptor responses. Experimental data for glycine derived from analysis of desensitization under these conditions was taken from Fig. 1 *B* and also included for comparison (☒).

included in these models, no difference between I_p and I_f EC_{50} values is observed if the degree of desensitization to a saturating concentration of glutamate reaches 48.1% and 30.2% for models 1 and 2, respectively (Fig. 6 *A*).

Comparison of the degree of desensitization modulated by glutamate to that of glycine

Fig. 5 *C* shows that analysis of simulated currents from different versions of model 1 yielded vastly different degrees of desensitization at saturating concentrations of glutamate. However, when background concentrations of glutamate were low (30 nM), the degrees of desensitization found for all three versions of model 1 were all ~80% (Fig. 5 *C*). One parameter that remained constant between the three simulations depicted in Fig. 5 *C* was the fourfold difference between K_1 and K_3. Thus, we reasoned that the degree of desensitization observed at low glutamate concentrations (30 nM) may be indicative of the difference in agonist-binding affinities represented by K_1 and K_3 (or K_2 and K_4).

To test this, the degree of desensitization was measured for simulated currents resulting from the application of 1 mM L-alanine in the continual presence of a background concentration of either 30 nM or 1 mM glutamate. The rate of return from the long-lived desensitized state in transition 5 was varied for models containing a twofold, fourfold, and eightfold difference in agonist-binding affinities (K_1 compared with K_3 or K_2 compared with K_4; see Table 1). Results from these simulations indicate that the degree of desensitization at low glutamate concentrations did not vary greatly with the degree of desensitization observed at maximal glutamate concentrations (Fig. 6 *B*). In addition, the degree of desensitization observed at low glutamate concentrations correlated with the degree of the affinity shift between the two agonist-binding states. For example, a twofold difference between K_1 and K_3 in model 1 yielded ~35–40% desensitization of the peak response when 30 nM glutamate was the background concentration; yet, a fourfold difference between K_1 and K_3 yielded approximately an 80% degree of desensitization (Fig. 6 *B*). However, note that the correlation between shifts in agonist affinity and the degree of desensitization at low concentrations of glutamate was model dependent. The degree of desensitization of experimental data acquired from a 1 mM pulse of L-alanine with a background concentration of 30 nM glutamate (Fig. 2 *D*) falls on the simulated curve for model 2, which contains a fourfold shift in glutamate affinities (Fig. 6 *B*). The real data also falls between the curves for model 1 containing either a twofold or fourfold difference in glutamate affinities.

For both models presented (Fig. 3), shifts in glutamate agonist affinities must be equivalent to shifts in glycine agonist affinity. Thus, Fig. 6 *B* can also be used to describe simulations in which 300 μM NMDA is pulsed in the continual presence of very low (30 nM) and saturating (10 μM) background concentrations of glycine. The degree of desensitization for 30 nM glycine determined from experimental data (Fig. 1 *B*) was similar to the degree of desensitization for 30 nM glutamate (Fig. 6 *B*) and suggests that the ratio of the low- and high-affinity states for glycine (K_4/K_2) may be similar to that of glutamate (K_3/K_1).

Fitting of glutamate dose-response data to models 1 and 2

Although analysis in Fig. 6 *B* indicates that the shift between high- and low-affinity states for glutamate binding may be three- to fourfold, these simulations were based on systematic variation of some of the rate constants (K_1, K_3, and K_5) whereas other rate constants (K_2, K_4, and K_6) were taken from the literature (Table 1). A better approach would be to search the parameter space by fitting the experimental data with models 1 and 2. Such an approach has been used previously for determining affinity shifts for desensitization modulated by glycine (Benveniste et al., 1990). We attempted to fit a prototypical raw data set composed of activation, desensitization, and deactivation kinetics observed in response to a pulse of 1 mM L-alanine in the continual presence of various background concentrations of glutamate with models 1 and 2. However, the kinetics of the decrease in current from I_p to I_f varied too greatly from cell to cell for us to determine whether one or two exponentials would best describe the current decay and prevented us from determining the decay time constant(s). Instead, the data sets of average I_p and I_f (Fig. 2 *C*) and the degree-of-desensitization data set (Fig. 2 *D*) were simultaneously fit with predicted values from each model.

All solution sets to the fitting procedure indicated that model 2 fit the data better than model 1 because model 2 had approximately a 1.5-fold lower SSE than model 1 (Fig. 7 *A*). All solution sets for a particular model yielded similar ratios between the low- and high-affinity states for glutamate binding. Model 1 yielded a ratio of K_3/K_1 of 3.4, whereas model 2 had a K_3/K_1 ratio of 8.8-fold (Fig. 7 *A*). These values were somewhat larger than the estimates from the simulations determined from Fig. 6 *B*.

The k_{off} values for transition types 1 and 3 were heavily dependent on the k_{on} values for those transitions. Therefore, the parameters from each solution set resulting from the fits described above were used in simulations of glutamate pulse experiments (Figs. 1 *C* and 2 *A*). The rising and decaying phases of current resulting from the addition and removal of glutamate in the continual presence of saturating glycine agonist could be compared with experimental data (Fig. 1 *C*). The rising phase was approximated with a single-exponential function for glutamate concentrations of 0.1–3 μM. A k_{on} value of 4 $\mu M^{-1}\ s^{-1}$ in model 2 yielded simulated responses whose $1/\tau_{on}$ analysis reasonably overlaid the experimental data (Fig. 7 *F*). The decaying phase of the NMDA receptor response measured upon removal of glutamate could not be fit with a single-exponential function. Analysis utilizing the sum of two exponential functions yielded slow and fast time constants (Fig. 7 *F*) with approximately equal contributions (amplitude data not shown). The rate constants for entry and exit from the long-lived desensitized state (transition 5) also indirectly affected the rate constants for glutamate dissociation. To limit the number of free parameters during the fit, k_{5off} was held constant during the fitting procedure, but these constant values were varied systematically between fits. Fits utilizing model 2 in which k_{5off} was fixed at 3.0 s^{-1} yielded the best overlay of the glutamate dissociation data (Fig. 7 *F*). Optimal fit parameters for model 2 are presented in Table 2, and their use in the simulation of desensitization resulting from a 1 mM L-alanine pulse with a given concentration of background glutamate (Fig. 7 *B*) is comparable to the experimental data (Figs. 1 *D* and 7).

Fitting of LCSS dose-response data to models 1 and 2

Finally, we wished to determine the magnitude of the agonist affinity shift when a different agonist was substituted for the background concentration of glutamate. L-Cysteine-S-sulfate (LCSS) was chosen as the glutamate agonist because it has apparent dissociation kinetics that can be measured with the whole-cell rapid perfusion system but has a 3.6-fold lower EC_{50} in comparison with glutamate (Patneau and Mayer, 1990). I_p and I_f dose-response curves (Fig. 8 *A*) measured in response to 1 mM L-alanine in the continual presence of a given background concentration of LCSS yielded EC_{50} values of 4.5 $\pm$ 1.5 and 4.8 $\pm$ 0.9 μM, Hill coefficients of 0.5 $\pm$ 0.1 and 0.8 $\pm$ 0.1, and I_{max} values of 116.4 $\pm$ 7.4% and 79.5 $\pm$ 3.6%, respectively ($n = 30$ cells). As expected, the degree of desensitization decreased with increasing background concentrations of LCSS, suggesting that a high and low LCSS affinity state may be present (Fig. 8 *B*). Analysis of the degree of desensitization with Eq. 4 yielded a D_{max} and D_{min} of 58.1 $\pm$ 3.4 and 26.0 $\pm$ 2.6%, respectively with a $CD_{1/2}$ of 2.6 $\pm$ 1.0 μM (fit not shown). The slope of the desensitization data was steep such that an accurate Hill coefficient could not be determined for the limited number of data points falling in that region. For this reason, n_D was constrained to 2.

The LCSS data presented in Fig. 8 were fit with models 1 and 2 utilizing I_p, I_f, and degree-of-desensitization data sets. As in the case of glutamate, fitting of the LCSS data yielded a 33% lower SSE for model 2 in comparison with model 1. On average, fitting to model 1 yielded a low to high binding affinity ratio (K_3/K_1) of 2.8 for LCSS, whereas

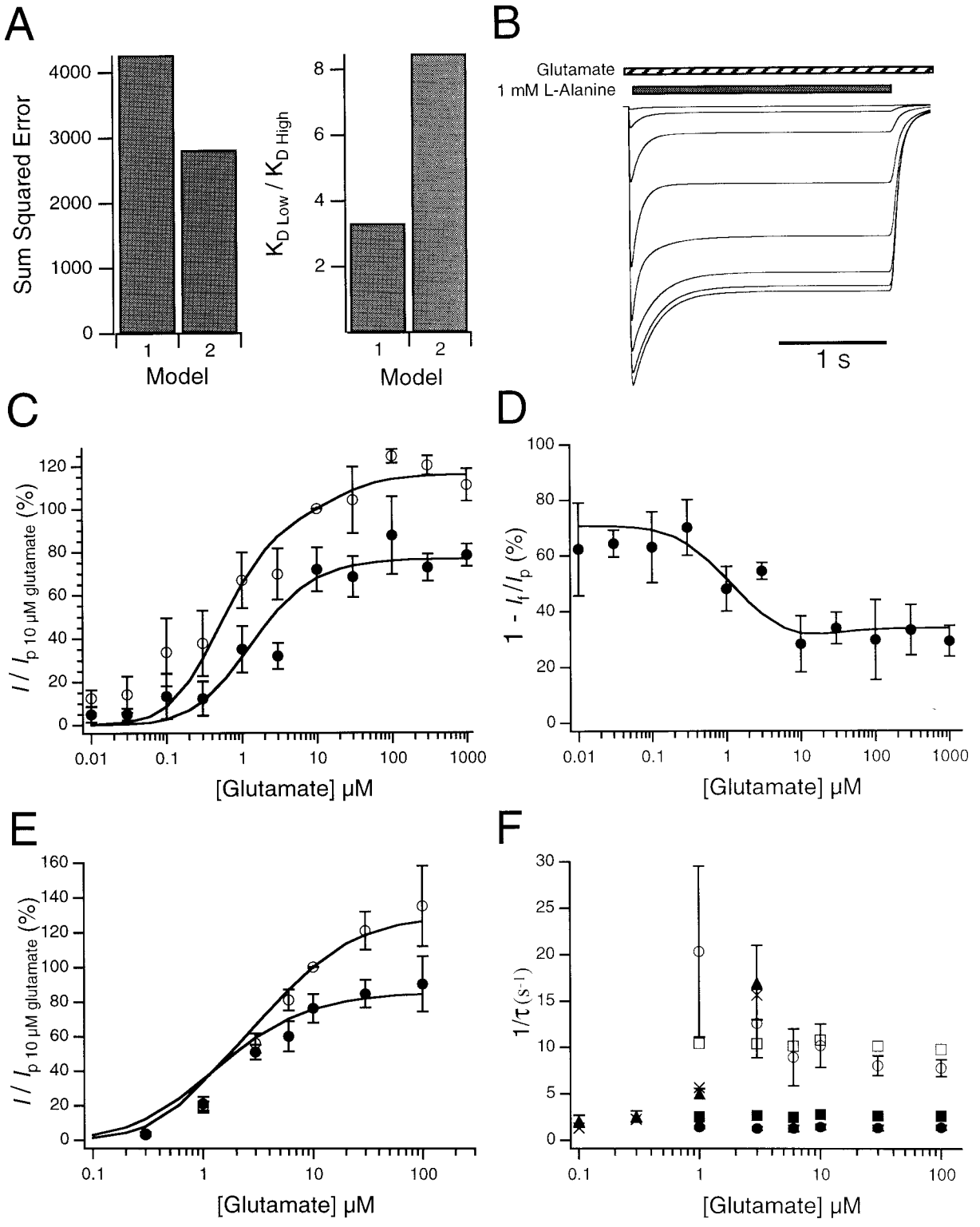

FIGURE 7 Fitting of glutamate dose-response and desensitization data to models 1 and 2. The best fits of glutamate data were obtained by simultaneous fitting of I_p, I_f, and degree-of-desensitization data. The fitted parameters were then utilized in other simulations to determine their overall applicability to the experimental data. (*A*) Comparison of fits of model 1 and model 2 indicated that model 2 had a lower SSE (*left panel*). The right panel indicates that the ratio of K_D values for low (K_{DLow}) and high (K_{DHigh}) affinity states for each agonist (K_3/K_1 or K_4/K_2) is also different between the two models. (*B*) Simulated currents of the best fit for model 2, which also yielded good overlap between simulations and experimental data presented in *E* and *F*. Fitted parameters can be found in Table 2. Background concentrations of glutamate depicted are 0.1, 0.3, 1, 3, 10, 30, 100, and 1000 μM (*C*) Overlay of experimental dose-response data for I_p and I_f (from Fig. 2 *C*) with the best fit of simulated I_p and I_f determined for model 2 (*smooth lines*). (*D*) Overlay

TABLE 2 Optimal rate constants for fitting model 2 to experimental data presented in Figs. 7 and 8

Transition*	Agonist	k_{on} (μM^{-1} s^{-1})	k_{off} (s^{-1})	k_{off}/k_{on}
1	Glutamate			
	Fig. 7	4.0†	0.97	0.24 μM
1	LCSS			
	Fig. 8	2.0‡	1.61	0.81 μM
2	L-Alanine			
	Fig. 7	1.7§	2.35	1.38 μM
	Fig. 8	1.7§	3.12	1.84 μM
3	Glutamate			
	Fig. 7	4.0†	8.25	2.06 μM
3	LCSS			
	Fig. 8	2.0‡	10.26	5.13 μM
4	L-Alanine			
	Figs. 7 and 8	1.7§	19.9§	11.7 μM
5	Agonist independent¶			
	Fig. 7	3.68	3.0†	0.82
	Fig. 8	2.81	3.0†	1.07
6	Agonist independent¶			
	Figs. 7 and 8	83.8‖	83.8‖	1.0

*Equivalent transition types are numbered are according to the scheme depicted in Fig. 3 *B*.
†Values were held constant during the fitting procedure but varied systematically between fittings.
‡This rate constant was arbitrarily chosen because no kinetic information was available. Thus, for LCSS data, only equilibrium dissociation constants ($K_D = k_{off}/k_{on}$) can be compared.
§Taken from Benveniste and Mayer (1991) and held constant for all simulations.
¶Agonist-independent k_{on} are in units of s^{-1}.
‖Taken from NMDA EPSC data of Lester and Jahr (1992) and held constant for all simulations.

fitting with model 2 yielded a ratio of 6.3 between the two binding affinity states (Table 2). Interestingly, when constraining the k_{off} values for L-alanine to those determined from fitting glutamate data (Table 2) and then refitting the data in Fig. 8, the SSE was only 18% higher than without this added constraint and yields a fit of the degree of desensitization that still overlays experimental data (Fig. 8 *B*). Under these constrained conditions, k_{1off} and k_{3off} were 1.41 and 12.0 s^{-1}, respectively.

DISCUSSION

The mechanistic connection between glutamate and glycine binding and NMDA receptor channel opening is poorly understood. Changes induced by glutamate agonist binding must trigger channel opening and may also weaken glycine binding site affinity (Benveniste et al., 1990; Vyklicky et al., 1990). The purpose of this study was to discern to what extent a similar weakening of glutamate binding affinity may occur. Addressing this problem can help us to understand whether glutamate and glycine agonists play symmetric or differential roles in the process of NMDA receptor activation.

Assaying for agonist affinity shifts by measuring desensitization of macroscopic currents

Two types of desensitization have been characterized for NMDA receptors. Desensitization of macroscopic currents in the presence of saturating concentrations of glutamate and glycine agonists has been described as glycine-independent or glycine-insensitive. This type of desensitization can be subdivided into calcium dependent (Krupp et al., 1996, 1999; Legendre et al., 1993; Medina et al., 1995) and independent components (Sather et al., 1990; Tong and Jahr, 1994), and key residues in the NR2 subunit control its magnitude (Krupp et al., 1998). Previously (Lester and Jahr, 1992), and in this paper (Fig. 3), this type of desensitization was modeled as entry of the channel into a relatively long-lived nonconducting state (i.e., transition 5).

A second type of desensitization could also be observed when glycine concentrations were subsaturating (Lerma et al., 1990; Vyklicky et al., 1990). The degree of desensitization elicited by an NMDA pulse decreased with an increasing background concentration of subsaturating glycine (Fig. 1 *B*). This type of desensitization could result if activation of NMDA receptors resulted in a weakening of glycine binding affinity (Benveniste et al., 1990). This affinity decrease causes glycine to re-equilibrate with its receptor at its lower affinity, thus lowering glycine binding site occupancy. In Fig. 2 *D* we show that the degree of desensitization of NMDA receptor responses to a pulse of L-alanine decreases as the concentration of glutamate increases between 3 and 100 μM. This may suggest that the glutamate binding affinity is also weakened upon activation of NMDA receptors.

To observe desensitization that can be attributed to a weakening of agonist binding affinity, the time constant of agonist re-equilibration with its low-affinity binding state after NMDA receptor activation (τ_{re}), must be several-fold larger than the time constant for solution exchange around

of experimental degree-of-desensitization data (from Fig. 2 *D*) with the best-fit parameters for simulated data using model 2. (*E*) Overlay of the experimental data for initial and steady-state pulse amplitudes from the glutamate pulse protocol (from Fig. 2 *A*) with the best-fit parameters for model 2. (*F*) The rising and declining phases of currents resulting from a glutamate pulse protocol (Fig. 1 *C*) were measured with one or two exponential time constants (τ), respectively. These values are compared with simulated currents subjected to the same type of analysis. ▲, $1/\tau$ measured from the rise in current from experimental data; ×, $1/\tau$ measured from the rise in current from simulated data utilizing the best fit from model 2; ○, $1/\tau_{fast}$ measured from the decay in current from experimental data; □, $1/\tau_{fast}$ measured from the decay in current from simulated data; ●, $1/\tau_{slow}$ measured from the decay in current from experimental data; ■, $1/\tau_{slow}$ measured from the decay in current from simulated data.

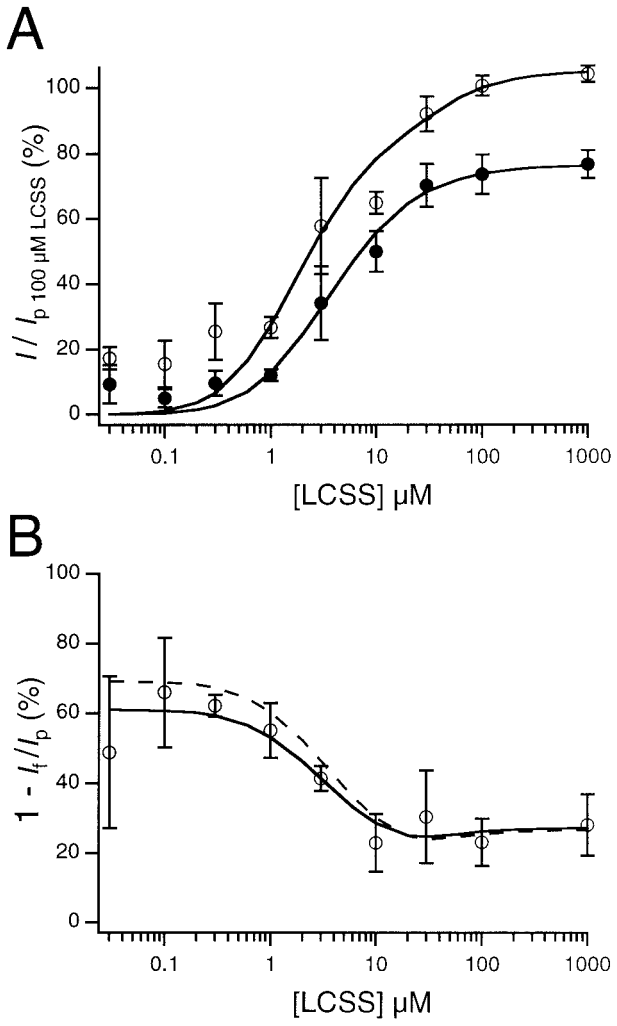

FIGURE 8 Fits of LCSS dose-response and desensitization data to models 1 and 2. (*A*) I_p (○) and I_f (●) responses of a 1 mM pulse of L-alanine in the presence of varying concentrations of LCSS. Responses are normalized to I_p of 100 μM LCSS. Simulated responses that best fit the experimental data for model 2 are depicted as solid lines, and best-fit parameters are presented in Table 2. (*B*) Comparison of the degree of desensitization with respect to LCSS concentration for experimental data (○) and the best fit using model 2 (——). Best-fit parameters for model 2 (Table 2) yielded a 6.3-fold difference between high- and low-affinity states for agonist binding. When L-alanine k_{off} values were kept constant at the best-fit values determined from fits to glutamate data (Fig. 7), the fits that resulted for LCSS data yielded simulated degree-of-desensitization data according to the dashed line.

the cell (τ_{ex}). τ_{re} is dependent on both the agonist association and dissociation rates. Recalling that the agonist association rate is concentration dependent, observation of desensitization resulting from a weakening of agonist affinity requires that the agonist be present in low concentrations and dissociate slowly from its binding site. Both glutamate and glycine, which have apparent dissociation time constants (τ_{off}) of several hundred milliseconds, fulfill this requirement whereas NMDA with a τ_{off} of ~20–40 ms does not (Benveniste et al., 1990; Benveniste and Mayer, 1991; Lester and Jahr, 1992; Priestley and Kemp, 1994; Sather et al., 1992).

Observation of desensitization that results from a weakening of agonist affinity also requires that agonists be applied in a particular order. Examination of data in which glutamate was pulsed with a constant background concentration of glycine (Figs. 1 *C* and 2 *A* and *B*) indicates no desensitization at low glutamate concentrations. In contrast, data acquired when L-alanine was pulsed in the presence of different background concentrations of glutamate (Figs. 1 *D* and 2, *C* and *D*) indicate the presence of desensitization at all glutamate concentrations. Glutamate must be pre-equilibrated with its receptor-binding site before triggering the molecular event that causes the rapid switch in glutamate-binding affinity to observe this type of desensitization. If glutamate pre-equilibration is not done (Fig. 1 *C*), then channel activation kinetics, which are limited by the rate of glutamate binding, can mask desensitization resulting from weakening of the glutamate-binding affinity.

Significant differences in I_p and I_f EC_{50} values can be indicative of a shift in agonist-binding affinity as has been observed previously (Fig. 2 *C* and Vyklicky et al., 1990). Analysis of I_p and I_f dose-response curves indicated a less than twofold change between I_p and I_f EC_{50} values for glutamate (Fig. 2 *C*) and no significant change between I_p and I_f EC_{50} values for LCSS (Fig. 8 *A*). Yet, Figs. 2 *D* and 8 *B* show that the degree of desensitization decreases as background glutamate or LCSS concentrations, respectively, increase. A decrease in the degree of desensitization with increasing background agonist concentration indicates that a component of desensitization can be attributed to the weakening of the background agonist binding affinity (comparison of Fig. 4 *C* with 5 *C*). In addition, Fig. 6 *A* indicates that a large degree of desensitization observed in the presence of saturating concentrations of background agonist can obscure differences between EC_{50} values for I_p and I_f dose-response curves. Thus, analysis of the relationship between the degree of desensitization and the background agonist concentration is probably a more reliable indicator for the existence of desensitization caused by a weakening of agonist affinity than standard I_p and I_f dose-response analysis.

Analysis of the degree of desensitization for simulations utilizing models in which K_3 was equal to $4K_1$ and also contained transition 5 (Fig. 5) yielded an interesting finding. As expected, the degree of desensitization measured when the concentration of background agonist was saturating increased as the ratio of k_{off}/k_{on} for transition 5 decreased (Table 1 and Fig. 5 *C*). However, the degree of desensitization measured when background agonist concentrations were very low did not change with changes in the transition 5 k_{off}/k_{on} ratio (Table 1; Fig. 5 *C*). When these simulations were run with different ratios of agonist binding affinities ($K_3 = 2K_1$, $K_3 = 4K_1$, or $K_3 = 8K_1$), the degree of desensitization observed at low background concentrations

of agonist increased as the ratio of K_3 to K_1 (or K_4 to K_2) increased (Fig. 6 *B*). This suggests that analysis of the degree of desensitization when the background concentration of agonist is low could be a good experimental measure of the ratio of high- to low-affinity agonist-binding states, because this measure is not very sensitive to desensitization caused by channels entering a long lived nonconducting state.

Mechanistic implications for NMDA receptor activation

The discovery that the degree of desensitization of NMDA receptor responses can be dependent on glutamate concentration complements earlier findings that the degree of desensitization can also be dependent on glycine concentration (Benveniste et al., 1990; Vyklicky et al., 1990). These observations reinforce the hypotheses that such desensitization results from a weakening of glutamate and glycine affinity that occurs upon NMDA channel activation. For symmetric cyclic models like those depicted in Fig. 3, the law of microscopic reversibility (Colquhoun and Hawkes, 1995) requires that changes in the ratio of affinity states for glutamate binding (K_3/K_1) must be accompanied by equivalent changes in the ratio of glycine agonist binding (K_4/K_2). Because the degree of desensitization measured for low background concentrations of agonist is indicative of the ratio of the high and low affinities of binding of that agonist, then both glutamate and glycine should yield similar degrees of desensitization and hence similar high- to low-affinity ratios, if NMDA receptors follow a cyclic, symmetric reaction scheme. Fig. 6 *B* shows that the degree of desensitization observed for a 1 mM pulse of L-alanine with a background concentration of 30 nM glutamate is similar to the degree of desensitization observed for a 300 μM pulse of NMDA with a background concentration of 30 nM glycine. This suggests that the ratio of low- to high-affinity glutamate binding and low- to high-affinity glycine binding is also similar and therefore supports a cyclic symmetric model for NMDA receptor activation.

In all trials, simultaneous fitting of I_p, I_f, and degree-of-desensitization data for glutamate (Fig. 7) and LCSS (Fig. 8) yielded lower SSE values for model 2 in comparison with model 1. This is in contrast to previously published results for pulses of 100 μM NMDA with differing background concentrations of glycine on mouse hippocampal neurons where a model similar to model 1 yielded the best fit (Benveniste et al., 1990). Differences between animal species and the type and concentration of agonists used between the two studies could possibly account for the discrepancy in model preference. Yet, other differences in the analysis done in the two studies also exist. Previously, transitions 5 and 6 (Fig. 3) were not explicitly modeled. Instead, the G_2RA_2 state was assumed to be the open state and analysis was limited to neurons that exhibited a minimal amount of desensitization under saturating agonist conditions such that transition 5 could be neglected. It should be noted that in this study, increasing or decreasing transition 6 k_{off} and k_{on} rate constants by 10-fold did change agonist dissociation constants resulting from the fitting procedure but not the ratio between the high-and low-affinity binding states for each agonist (data not shown).

Mutational analysis of recombinant NMDA receptors suggests that glutamate and glycine agonists bind at independent receptor sites (Anson et al., 1998; Hirai et al., 1996; Kuryatov et al., 1994; Laube et al., 1997); yet, the law of microscopic reversibility dictates that reaction rate constants in a cyclic reaction scheme for activation are not entirely independent. According to the law of microscopic reversibility, the ratio of microscopic K_D values between high-affinity (K_1) and low-affinity (K_3) binding states in a cyclic model should be constant for any glutamate agonist if the same glycine agonist (with constant K_2 and K_4 values) is always used. In contrast, one expects that any glutamate agonist would have its own intrinsic high- and low-affinity K_D values (K_1 and K_3), indicating that the ratio of K_1 to K_3 could vary substantially for different glutamate agonists. This contradiction can be resolved by postulating that K_2 and K_4 values for a particular glycine agonist can be slightly modified so that the ratio of K_4 to K_2 matches the ratio of K_3 to K_1 for a particular glutamate agonist. Conversely, K_1 and K_3 values for a particular glutamate agonist can also be slightly modified so that the ratio of K_3 to K_1 matches the ratio K_4 to K_2 for a particular glycine agonist. This would suggest that although the microscopic high- and low-affinity binding constants for both glutamate and glycine agonists can vary substantially, the ratio of the high- to low-affinity binding constants will not vary greatly. The ratio of high to low binding affinities by fitting model 2 to dose-response and degree-of-desensitization data was 8.5 and 6.3 for glutamate and LCSS, respectively (Figs. 7 and 8). These values are not strikingly different. These data suggest that the ratios of high to low binding affinities for glutamate and glycine agonists are interdependent. Previously, it has been shown that both glutamate and glycine agonist dissociation rates depend on the co-agonist present (Priestley and Kemp, 1994). Slower glutamate dissociation was correlated with the presence of a higher-affinity full glycine co-agonist. Also, slower glycine dissociation was correlated with the presence of a higher-affinity glutamate co-agonist (Priestley and Kemp, 1994). Such a functional linkage between the glutamate- and glycine-binding sites could result from a direct allosteric interaction between the two binding sites or by having common molecular elements in the pathway to channel activation and opening. Currently, we are trying to distinguish whether the molecular events that cause the apparent affinity switch for agonist binding could be the act of co-agonist binding as implied by the models illustrated above, channel opening, and/or ion permeation.

We thank Professor Ilana Lotan and Dr. Nitza Ilan for their helpful comments on this manuscript.

This research was supported by grant 96–00245 from the United States-Israel Binational Science Foundation (BSF), Jerusalem, Israel, and grant 572/99–16.0 from the Israel Science Foundation.

REFERENCES

Anson, L. C., P. E. Chen, D. J. A. Wyllie, D. Colquhoun, and R. Schoepfer. 1998. Identification of amino acid residues of the NR2A subunit that control glutamate potency in recombinant NR1/NR2A NMDA receptors. *J. Neurosci.* 18:581–589.

Benveniste, M., J. Clements, L. Vyklicky, Jr., and M. L. Mayer. 1990. A kinetic analysis of the modulation of *N*-methyl-D-aspartic acid receptors by glycine in mouse cultured hippocampal neurones. *J. Physiol. (Lond.).* 428:333–357.

Benveniste, M., and M. L. Mayer. 1991. Kinetic analysis of antagonist action at *N*-methyl-D-aspartic acid receptors: two binding sites each for glutamate and glycine. *Biophys. J.* 59:560–573.

Clements, J. D., and G. L. Westbrook. 1991. Activation kinetics reveal the number of glutamate and glycine binding sites on the *N*-methyl-D-aspartate receptor. *Neuron.* 7:605–613.

Clements, J. D., and G. L. Westbrook. 1994. Kinetics of AP5 dissociation from NMDA receptors: evidence for two identical cooperative binding sites. *J. Neurophysiol.* 71:2566–2569.

Colquhoun, D., and A. G. Hawkes. 1995. The principles of the stochastic interpretation of ion-channel mechanisms. *In* Single-Channel Recording. B. Sakmann and E. Neher, editors. Plenum Press, New York. 397–482.

Dingledine, R., K. Borges, D. Bowie, and S. F. Traynelis. 1999. The glutamate receptor ion channels. *Pharmacol. Rev.* 51:7–61.

Guthrie, P. B., D. E. Brenneman, and E. A. Neale. 1987. Morphological and biochemical differences expressed in separate dissociated cell cultures of dorsal and ventral halves of the mouse spinal cord. *Brain Res.* 420:313–323.

Hirai, H., J. Kirsch, B. Laube, H. Betz, and J. Kuhse. 1996. The glycine binding site of the *N*-methyl-D-aspartate receptor subunit NR1: identification of novel determinants of co-agonist potentiation in the extracellular M3–M4 loop region. *Proc. Natl. Acad. Sci. U.S.A.* 93:6031–6036.

Huettner, J. E. 1989. Indole-2-carboxylic acid: a competitive antagonist of potentiation by glycine at the NMDA receptor. *Science.* 243:1611–1613.

Kleckner, N. W., and R. Dingledine. 1988. Requirement for glycine in activation of NMDA-receptors expressed in *Xenopus* oocytes. *Science.* 241:835–837.

Krupp, J. J., B. Vissel, S. F. Heinemann, and G. L. Westbrook. 1996. Calcium-dependent inactivation of recombinant *N*-methyl-D-aspartate receptors is NR2 subunit specific. *Mol. Pharmacol.* 50:1680–1688.

Krupp, J. J., B. Vissel, S. F. Heinemann, and G. L. Westbrook. 1998. N-terminal domains in the NR2 subunit control desensitization of NMDA receptors. *Neuron.* 20:317–327.

Krupp, J. J., B. Vissel, C. G. Thomas, S. F. Heinemann, and G. L. Westbrook. 1999. Interactions of calmodulin and alpha-actinin with the NR1 subunit modulate Ca^{2+}-dependent inactivation of NMDA receptors. *J. Neurosci.* 19:1165–1178.

Kuryatov, A., B. Laube, H. Betz, and J. Kuhse. 1994. Mutational analysis of the glycine-binding site of the NMDA receptor: structural similarity with bacterial amino acid-binding proteins. *Neuron.* 12:1291–1300.

Laube, B., H. Hirai, M. Sturgess, H. Betz, and J. Kuhse. 1997. Molecular determinants of agonist discrimination by NMDA receptor subunits: analysis of the glutamate binding site on the NR2B subunit. *Neuron.* 18:493–503.

Legendre, P., C. Rosenmund, and G. L. Westbrook. 1993. Inactivation of NMDA channels in cultured hippocampal neurons by intracellular calcium. *J. Neurosci.* 13:674–684.

Lerma, J., R. S. Zukin, and M. V. Bennett. 1990. Glycine decreases desensitization of *N*-methyl-D-aspartate (NMDA) receptors expressed in *Xenopus* oocytes and is required for NMDA responses. *Proc. Natl. Acad. Sci. U.S.A.* 87:2354–2358.

Lester, R. A., and C. E. Jahr. 1992. NMDA channel behavior depends on agonist affinity. *J. Neurosci.* 12:635–643.

Mayer, M. L., L. Vyklicky, Jr., and J. Clements. 1989. Regulation of NMDA receptor desensitization in mouse hippocampal neurons by glycine. *Nature.* 338:425–427.

Medina, I., N. Filippova, G. Charton, S. Rougeole, Y. Ben-Ari, M. Khrestchatisky, and P. Bregestovski. 1995. Calcium-dependent inactivation of heteromeric NMDA receptor-channels expressed in human embryonic kidney cells. *J. Physiol. (Lond.).* 482:567–573.

Nahum-Levy, R., L. H. Fossom, P. Skolnick, and M. Benveniste. 1999. Putative partial agonist 1-aminocyclopropanecarboxylic acid acts concurrently as a glycine-site agonist and a glutamate-site antagonist at *N*-methyl-D-aspartate receptors. *Mol. Pharmacol.* 56:1207–1218.

Ozawa, S., H. Kamiya, and K. Tsuzuki. 1998. Glutamate receptors in the mammalian central nervous system. *Prog. Neurobiol.* 54:581–618.

Patneau, D. K., and M. L. Mayer. 1990. Structure-activity relationships for amino acid transmitter candidates acting at *N*-methyl-D-aspartate and quisqualate receptors. *J. Neurosci.* 10:2385–2399.

Press, W. H., S. A. Teukolsky, W. T. Vetterling, and B. P. Flannery. 1992. Downhill simplex method in multidimensions. *In* Numerical Recipes in FORTRAN, 2nd ed. Cambridge University Press, Cambridge. 402–406.

Priestley, T., and J. A. Kemp. 1994. Kinetic study of the interactions between the glutamate and glycine recognition sites on the *N*-methyl-D-aspartic acid receptor complex. *Mol. Pharmacol.* 46:1191–1196.

Rosenmund, C., Y. Stern-Bach, and C. F. Stevens. 1998. The tetrameric structure of a glutamate receptor channel. *Science.* 280:1596–1599.

Sather, W., S. Dieudonne, J. F. MacDonald, and P. Ascher. 1992. Activation and desensitization of *N*-methyl-D-aspartate receptors in nucleated outside-out patches from mouse neurones. *J. Physiol. (Lond.).* 450: 643–672.

Sather, W., J. W. Johnson, G. Henderson, and P. Ascher. 1990. Glycine-insensitive desensitization of NMDA responses in cultured mouse embryonic neurons. *Neuron.* 4:725–731.

Tong, G., and C. E. Jahr. 1994. Regulation of glycine-insensitive desensitization of the NMDA receptor in outside-out patches. *J. Neurophysiol.* 72:754–761.

Vyklicky, L., Jr., M. Benveniste, and M. L. Mayer. 1990. Modulation of *N*-methyl-D-aspartic acid receptor desensitization by glycine in mouse cultured hippocampal neurones. *J. Physiol. (Lond.).* 428:313–331.